CHAPTER VI

PHASE DIAGRAMS INVOLVING A_d AND A_1 PHASES

6.1 INTRODUCTION

As described in chapter IV, the origin of polymorphism of smectic A phase is due to a competition between ordering at two different length scales. When the competing lengths are molecular length ℓ and the length ℓ' of a pair of molecules ($\ell < \ell' < 2R$) one encounters a situation leading to an A_d-A_1 transition. On the other hand, competition between ℓ' and 2ℓ leads to an A_d-A_2 transition. As shown in chapter IV, under certain circumstances, the first order A_d-A_2 transition ends as a gas-liquid type of critical point beyond which A_d evolves continuously into A_2 phase. It has also been shown experimentally[1] that under certain other circumstances an incommensurate phase (A_{ic}) can intervene between the A_d and A_2 phases.

The situation concerning A_d-A_1 transitions has been dealt with theoretically by Prost and Toner[2] using the dislocation loop approach. This theory predicts some novel features concerning the terminus of the A_d-A_I transition boundary, only some of these having been observed experimentally so far. We shall briefly discuss the important aspects of the theory in §6.2 of this chapter. The previously reported experimental work concerning the A_d-A_1 transi-

tions is summarised in 56.3. Finally in §6.4 we shall present the experimental phase diagrams obtained by us which reproduce qualitatively some of the topological features predicted by the theory.

6.2 DISLOCATION LOOP THEORY OF THE NEMATIC ISLAND IN A SMECTIC SEA

Recently, Prost and Toner[2] have developed a dislocation loop theory of the nematic-smectic A transition. It predicts the existence of two interesting possible situations near an expected A_d-A_1 critical point. This theory essentially consists of two parts, in the first part Prost and Toner use the Landau theory similar to that proposed by Barois, Prost and Lubensky[3] to show that an A_d-A_1 critical point can exist in a way similar to the A_d-A_2 critical point discussed earlier. The second part of the theory explains through a fluctuation-corrected mean-field theory the possibility of the existence of a smal! nematic island at the termination of the A_d-A_1 boundary. The physics of the mechanism can be explained in terms of unbinding of dislocation loops. This unbinding occurs when the entropy gained by proliferating these loops through the smectic reduces the total free energy more than the increase[4] caused by the energy of the loop. Since the smectic layer compression elastic constant $\bar{B}$ is expected to vanish at the A_d-A_1 critical point (in close analogy with the divergence of compressibility of liquid at the liquid-gas critical

point), the elastic energy of the dislocation loops should have a minimum near the critical point. If this minimum of the elastic energy is below the threshold energy required for loop unbinding, in that case the loops will unbind and consequently a nematic island will appear. However, Prost and Toner point out clearly that this picture is certainly not the universal one. Although, the energy of dislocation loop shows a local minimum near the critical point, its value at that minimum need not essentially be zero. In that case the A_d-A_l first order boundary can, in fact, end as a critical point without the occurrence of a nematic island. In other words, Prost and Toner predict that in some materials the termination of A_d-A_l first order boundary can be a nematic island while in other materials it could just be a critical point.

Using the mean field approach, Prost and Toner have predicted a variety of phase diagrams involving A_d-A_l phase boundary. This was done by expanding the free energy density f in powers of the two spatially varying order parameters $\psi_l(\bar{r})$ and $\psi_d(\bar{r})$ that represent respectively the monolayer and partial bilayer order. Since they were interested in transitions into and between A_1 and A_d states, they considered the case in which both ψ_l and ψ_d order at the same wavevector $\bar{q}=q\hat{z}$, where $\hat{z}$ points along the director. in the 'nematic phase; i.e., $\psi_l(\bar{r}) = |\psi_l| e^{i(qz+\phi_l)}$; $\psi_d(\bar{r}) = |\psi_d| e^{i(qz+\phi_d)}$ As usual only those terms in f up to fourth order in ψ_l and

ψ_d have been retained. The resultant free energy density, upon minimizing over the phases ψ_1 and @ reads:

$$f = r_1\frac{1}{2}|\psi_1|^2 + \frac{C_1}{2}(q^2-q_1^2)^2|\psi_1|^2 + \frac{U_1}{4}|\psi_1|^4$$
$$+\frac{1}{2}r_d|\psi_d|^2+\frac{1}{2}C_d(q^2-q_d^2)^2|\psi_d|^2 + \frac{U_d}{4}|\psi_d|^4$$
$$- |\psi_1|\,|\psi_d| + \frac{U_d}{2}|\psi_1|^2\,|\psi_d|^2 \quad , \qquad (1)$$

where the wavevectors q_1 and q_d correspond to the optimal lengths ℓ and ℓ' ($q_1=2\pi/\ell$; $q_d=2\pi/\ell'$; typically $\ell'=1.3\ell$), and the terms such as $W_1\psi_1\psi_d^*|\psi_d|^2$ and $W_2\psi_d\psi_1^*|\psi_1|^2$ have been ignored for the sake of simplicity. Prost and Toner have verified that their results for the possible topologies of the phase diagram are stable against small non-zero values of W_1 and W_2. They, then sought to determine the phase diagram in the r_1-r_d plane, which presumably maps continuously onto, say, the temperature-concentration plane of a real experiment. This phase diagram follows from minimizing f over all possible values of q, ψ_1 and ψ_d. Different local minima of f then correspond to different phases - the places where these minima cross are the phase boundaries.

A straightforward minimization with respect to q yields (after the variable change: $\psi_1 = S\cos\theta/\sqrt{C_1}$, $\psi_d = S\sin\theta/\sqrt{C_d}$)

$$q_m^2 = q_l^2 \cos^2\theta + q_d^2 \sin^2\theta$$

and

$$f = \frac{I}{2} r(\theta) S^2 + \frac{U(\theta)}{4} S^4$$

with $r(\theta) \equiv \bar{r} - \mu \sin(2\theta) + \cos(2\theta)\delta r - K\cos^2 2\theta$ and $U(\theta) = U + 2\delta U \cos 2\theta + U' \cos^2 29$, where we have defined

$$\bar{r} \equiv \frac{1}{2}\left(\frac{r_l}{C_l} + \frac{r_d}{C_d}\right) + K, \quad \mu \equiv \frac{\lambda}{(C_l C_d)^{1/2}}, \quad K \equiv (q_d^2 - q_l^2)^2/4$$

$$\delta r \equiv \frac{1}{2}\left(\frac{r_l}{C_l} - \frac{r_d}{C_d}\right), \quad \bar{U} \equiv \frac{}{C_l^2} + \frac{U_d}{C_d^2} + \frac{2u_{ld}}{C_l C_d} \Big/ 4$$

$$\delta U \equiv \left(\frac{U_l}{C_l^2} - \frac{U_d}{C_d^2}\right)/4, \quad U' \equiv \left(\frac{U_l}{C_l^2} + \frac{U_d}{C_d^2} - \frac{2U_{ld}}{C_l C_d}\right) / 4$$

The nematic-smectic transition occurs when the smallest value of $r(\theta)$ vanishes, that is

$$r(\theta) = \frac{\partial r(\theta)}{\partial \theta} = 0 \quad . \tag{2}$$

On the smectic side, the minimization of the free energy over ψ gives

$$f = -\frac{r^2(\theta)}{4U(\theta)} \quad . \tag{3}$$

The first order S_A-S_A transitions occur at those values of r and

δr for which minima of f at two different values of **0** become equal.

The different possible topologies are given in Figs. 6.1 -*6.5.* In all cases the nematic-smectic A transition line obtained by solving equation (2) is given in a parametric form represented by :

$$\bar{r} = \frac{\mu}{\sin 2\theta} - K \cos^2 \theta$$

$$r = -\mu \cot 2\theta + 2K \cos 2\theta \quad . \qquad (4)$$

For $\mu > 2K$ the $N\text{-}S_A$ boundary and its derivative are continuous. The first order $S_A\text{-}S_A$ line, if it exists, does not intersect the $N\text{-}S_A$ one, which implies the existence of (at least) one isolated critical point. The phase diagram is particularly simple to calculate if $\delta U=0$, for then it must be symmetric in δr. The five possible topologies that emerge after calculation fall into two classes :

1 For $\mu > 2K$, there is no S_A-nematic bicritical point.

(a) If $U' > 0$ there is just an A-N boundary, but no A-A transition line. The A_1 phase goes continuously to A_d phase without transition, i.e., the area surrounding the A-N boundary is nothing but critical region (Fig. 6.1);

(b) If $U' < 0$, the situation leads to a phase diagram shown in Fig.6.2, i.e., the A-N boundary is separated from the $A_1\text{-}A_d$ line by a region wherein A_d goes continuously to A_1 (critical region). Also, the $A_1\text{-}A_d$ boundary terminates at the critical

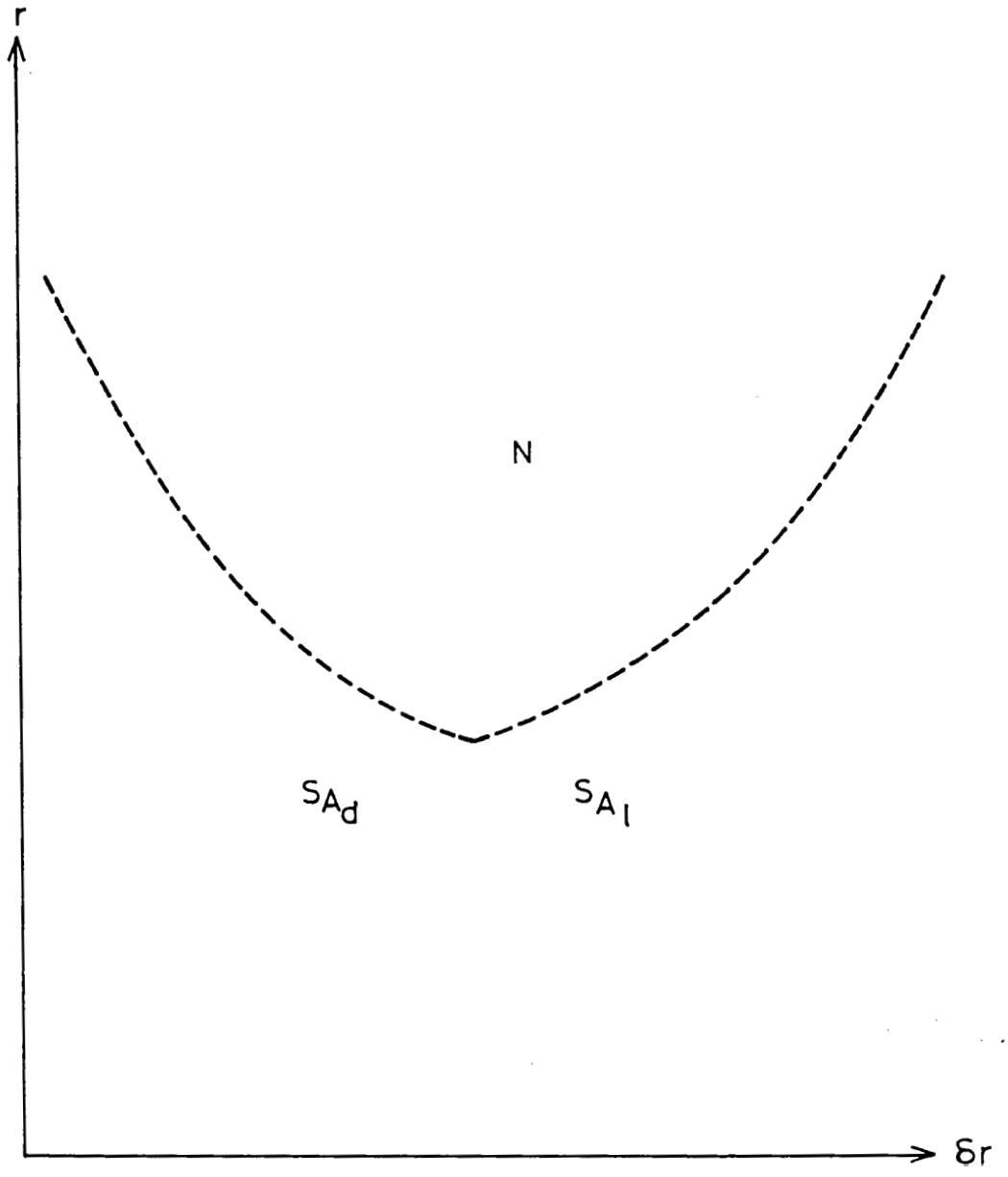

Figure 6.1

Mean-field phase diagram for the parameters μ, K, U and U' in the range $\mu > 2K$, $U' > 0$. Dashed line denotes second order phase transition. N = nematic, S_A = smectic A (Ref. 2).

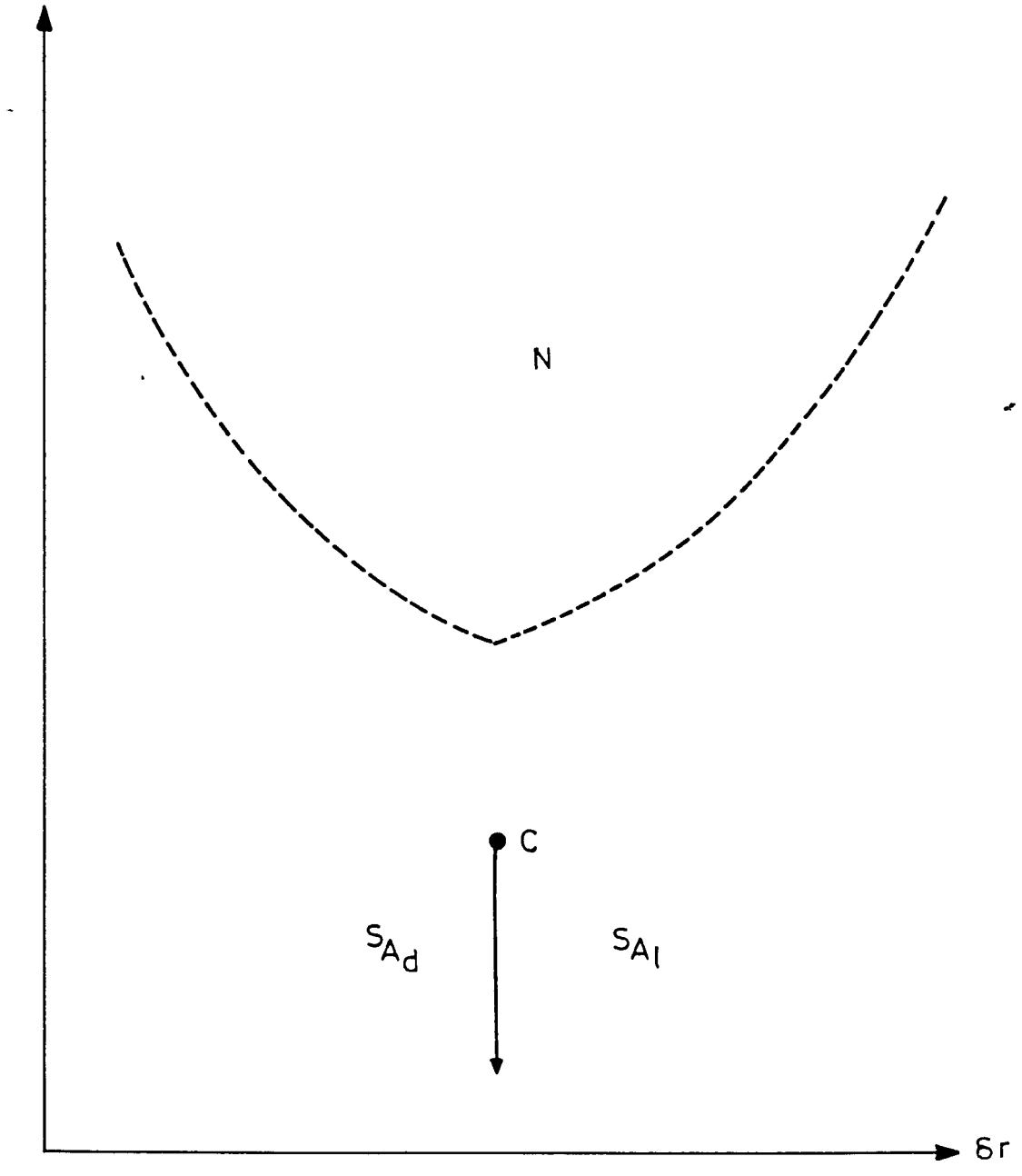

Figure 6.2

Mean-field phase diagram for the parameters μ, K, U and U' in the range $\mu > 2K$, $U' < 0$. Dashed and full lines represent second or first order phase boundaries (Ref. 2).

point C in one direction while it continues to ∞ in the other direction.

2 For $\mu < 2K$, the A-N boundary now meets the first order A_d-A_l line leading to a N-A_d-A_l bicritical point (B). Under this condition there are three possibilities: -

a) If $U' > 0$, and $(U/U') > (2K-\mu)/\mu$, there is only one critical point C in addition to the bicritical point. There is a critical point for A_d-A_l line C (Fig.6.3).

b) If $U' > 0$ and $(U/U') < (2K-\mu)/\mu$, there are two such critical points (Fig.6.4) in addition to a triple point T.

c) If $U' < 0$, $\mu < 2K$, the first order A_l-A_d boundary extends all the way from the bicritical point to infinity (Fig.6.5).

Thus the mean-field theory predicts the existence of a variety of experimental systems displaying first order smectic A_l-smectic A_d lines that do not intersect the S_A-N phase boundary. But the mean-field theory does not predict the existence of nematicislands in phase diagrams. Prost and Toner argue that this phenomenon (of observing nematic island) is caused due to fluctuation effect. Using fluctuation corrected mean-field theory they predict a phase diagram of the type (Fig.6.6). There are several important features of this phase diagram.

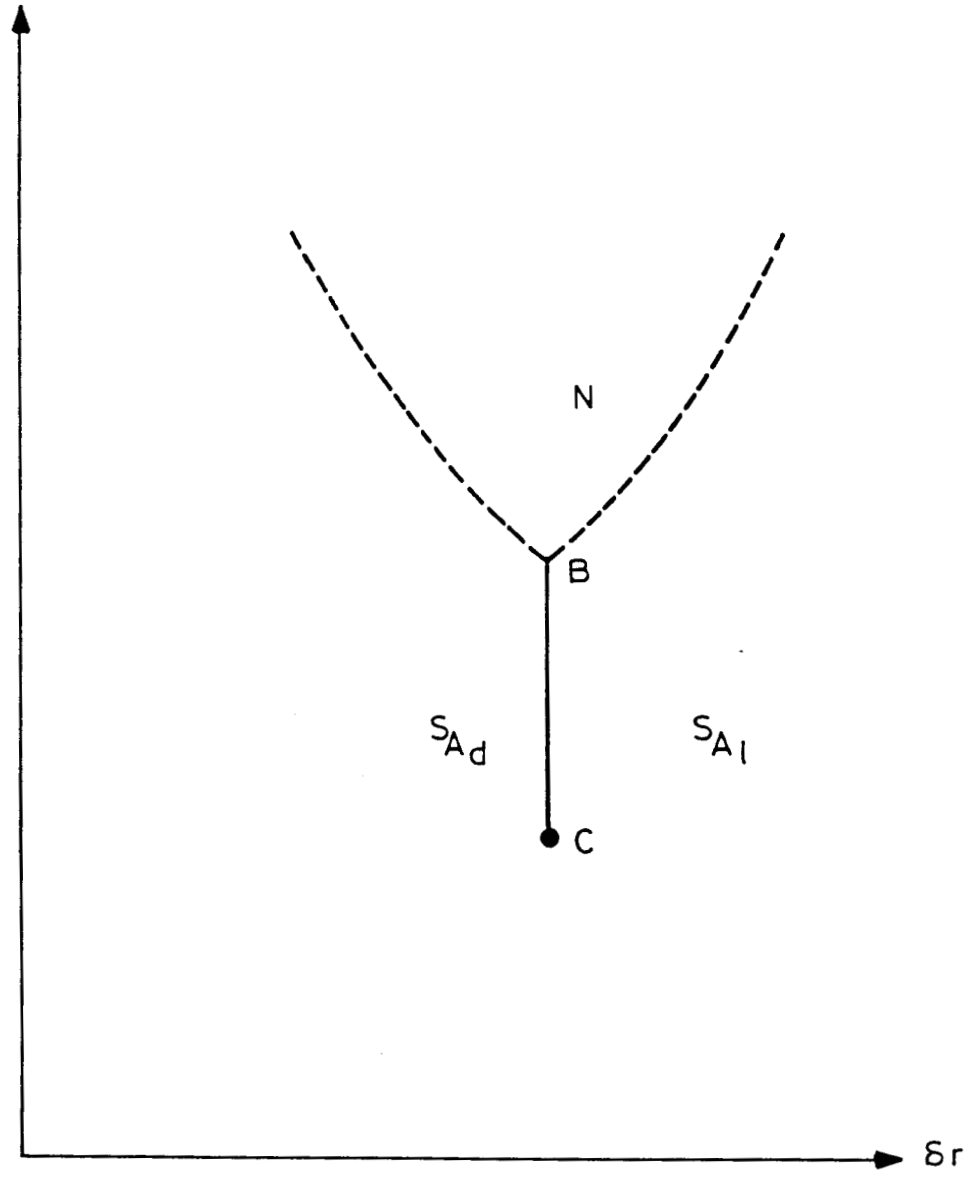

Figure 6.3

Mean-field phase diagram for parameters μ, K, U and U' in the range $\mu<2K$, $U'>0$, $\frac{U}{U'}, > \frac{2K}{\mu} - 1$. (See also Figure legend of 6.2) (Ref. 2).

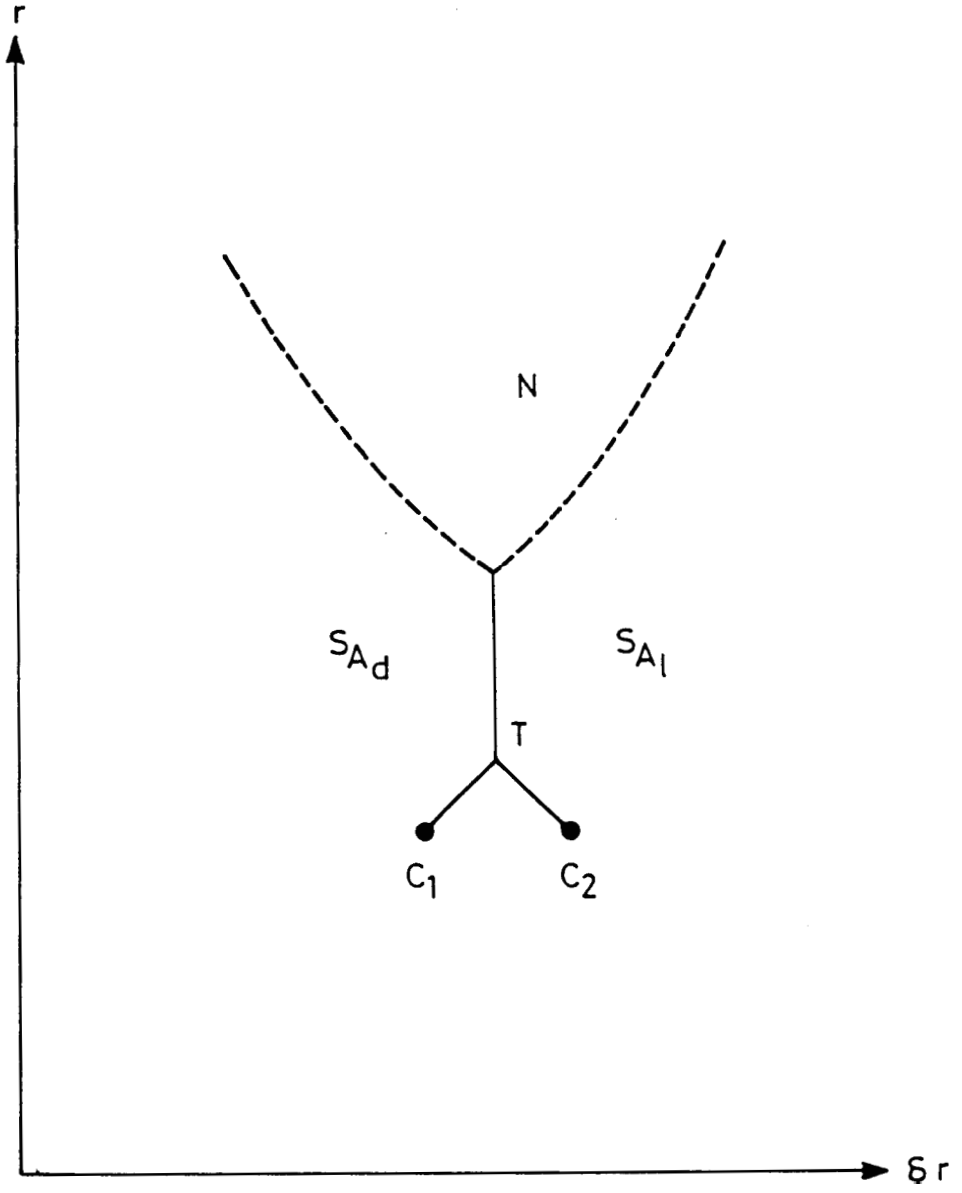

Figure 6.4

Mean-field phase diagram for parameters μ, K, U and U' in the range, $\mu < 2K$, $U' > 0$, $\frac{U}{U'} < \frac{2K}{\mu} - 1$. (See also Figure Legend of 6.2) (Ref. 2).

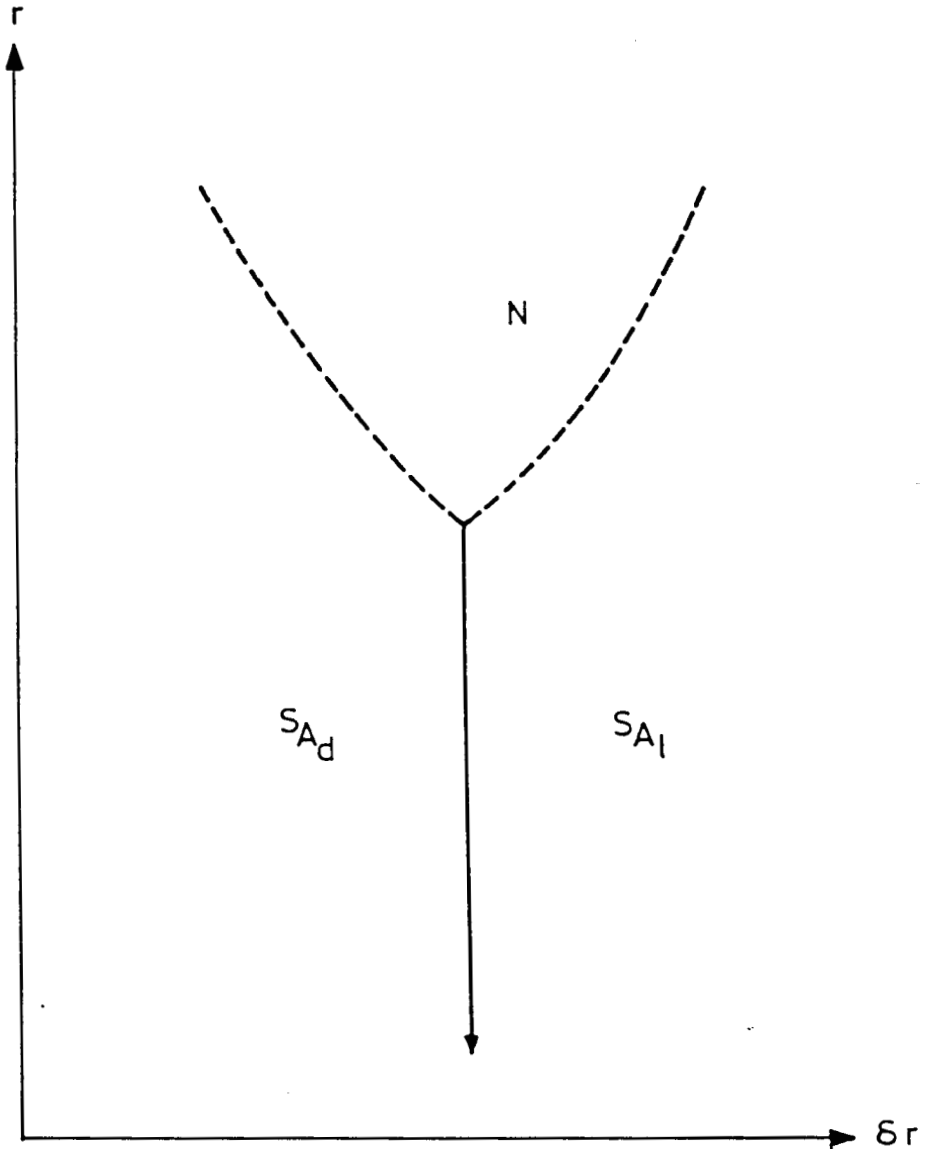

Figure 6.5

Mean-field phase diagram for parameters μ, K, U and U' in the range, $\mu < 2K$, $U' < 0$. (See also Figure legen 6.2) (Ref. 2).

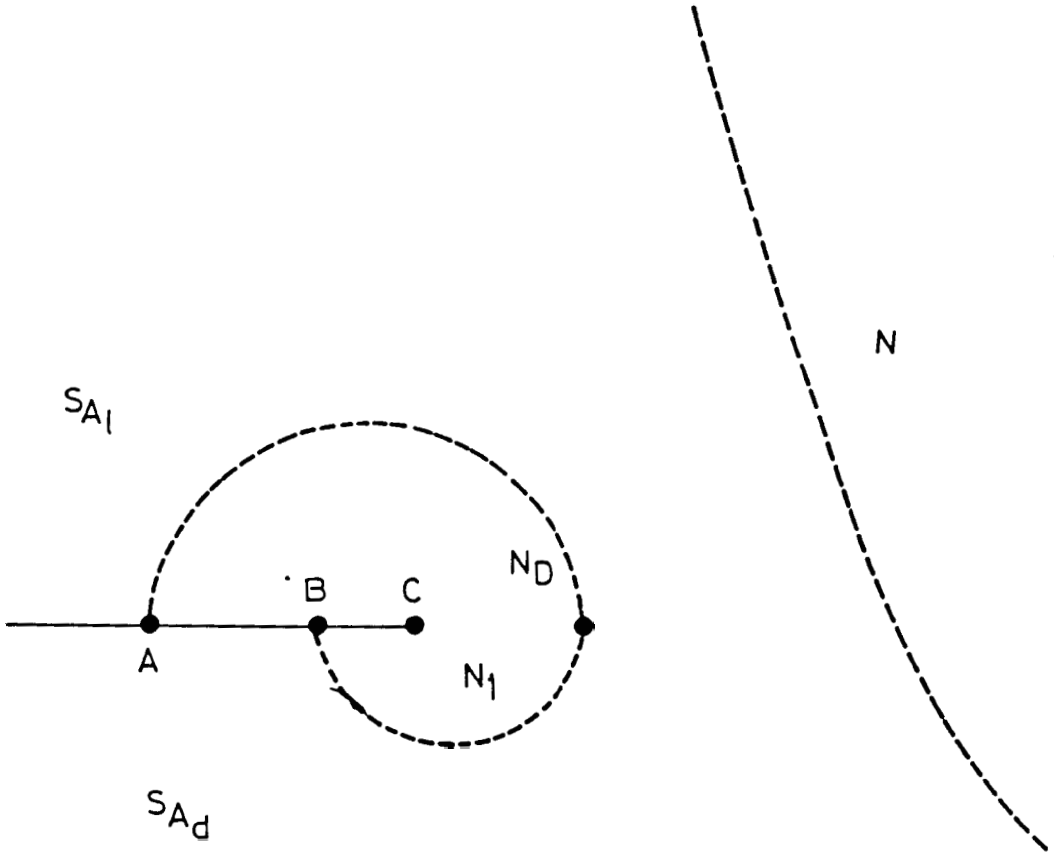

Figure 6.6

Experimentally observed phase diagram in $S_{A_l} - S_{A_d}$ mixtures. The resolution of the actual experiments was insufficient to distinguish between the critical end points A and B, which are predicted by the theory. (Ref. 2).

1) A_d-A_l boundary ends as a nematic island which is separated from a 'main domain' of nematic.

2) There is no N-A_d-A_l bicritical point, but instead there are two critical end points A and B (shown in Fig.6.6).

3) Perhaps the most interesting prediction of this phase diagram is the occurrence of two types of nematic phases, N_d and N_l over a certain range in the phase diagram. The N_d-N_l phase boundary which exists ends as a nematic-nematic critical point C. The absence of long range layer fluctuations implies that this N_d-N_1 critical point should fall into the universality class of a liquid-gas critical point.

Prost and Toner also point out that by varying different parameters in their theory it is possible to predict a large number of topologically distinct phase diagrams, the possibility of nematic island merging with the main domain nematic leading to a phase diagram of type shown in Fig.6.7 is also considered. We shall in the next section briefly summarize the earlier work on experimental phase diagrams exhibiting A_d-A_l phases.

6.3 EARLIER ATTEMPTS TO OBSERVE A_d-A_l CRITICAL POINT

The first observation of nematic island in a smectic sea was by Cladis and Brand,[5] who reported that in the temperature-con-

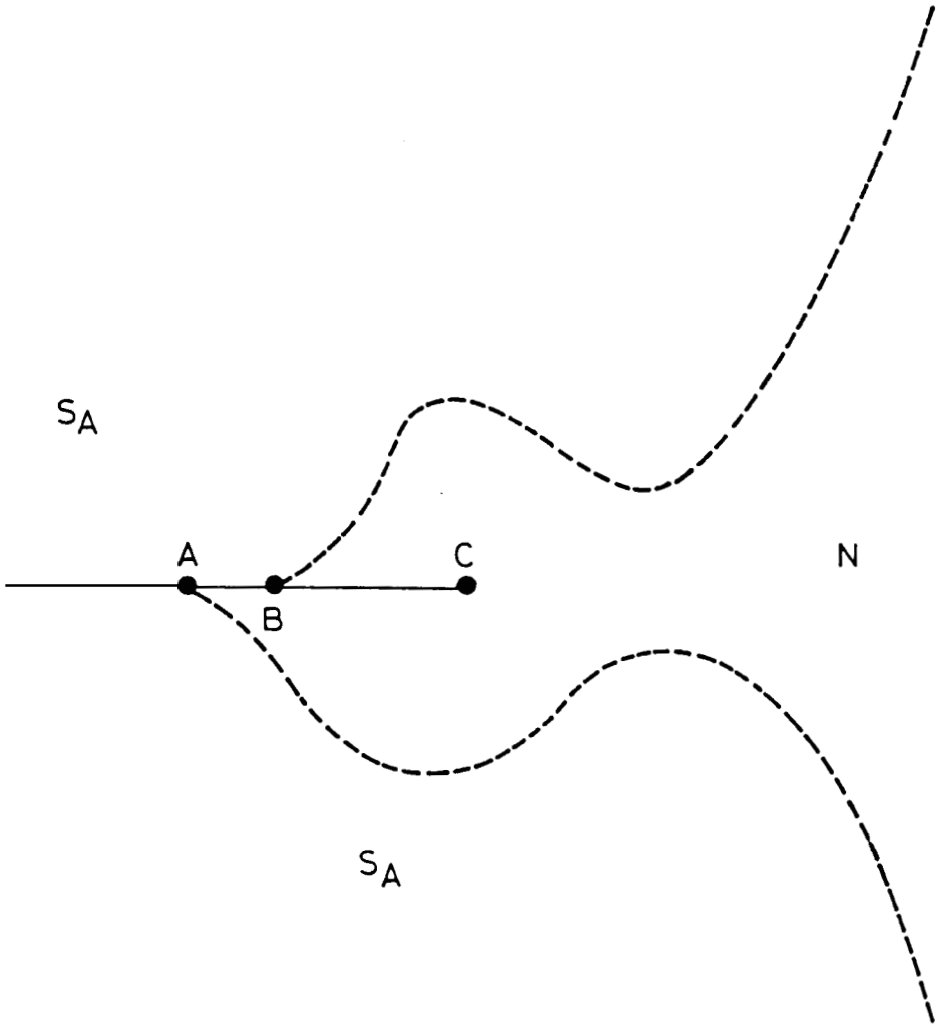

Figure 6.7

Topology when the nematic island merges with the main domain (Ref. 2).

centration diagram of 4-n-nonyloxybiphenyl-4'-cyanobenzoate (9OBCB) and 1-4-di(4-methylhexyloxybenzoate) 2-chlorophenyl (4M6Cl), a cholesteric phase appears as an island surrounded by smectic phases (Fig.6.8). More recently, Hardouin et al.[6] have given a series of phase diagrams which reveal that a close loop of nematic island and a bicritical point ($N-A_d-A_l$ point) are two topologies connected in a given T-X plane. These phase diagrams are reproduced in Fig. 6.9(a-d). In particular, mention may be made of their binary phase diagram of compounds A and B which results in a nematic bubble (Fig.6.9d). From the Xray experiments conducted on several binary mixtures (of A and B), Hardouin et al. showed that, beyond the region of existence of nematic bubble, A_l phase continuously goes to A_d phase without a transition. Cladis and Brand[5] had also reported exactly similar Xray results for binary mixtures of 9OBCB/4M6Cl. However it should be pointed out that neither the experiments of Cladis and Brand nor that of Hardouin et al. showed the existence of a phase transition between the two types of nematic phases (N_d and N_l). The topological features associated with theoretical predictions (Fig.6.6), namely, the existence of two distinct critical end points was also not observed. It is therefore of interest to make a qualitative study of phase diagrams involving A_d and A_l phases to see if some of the topological features predicted by theory can be reproduced by experiments. The results of experimental investigations undertaken by us are presented in the next section.

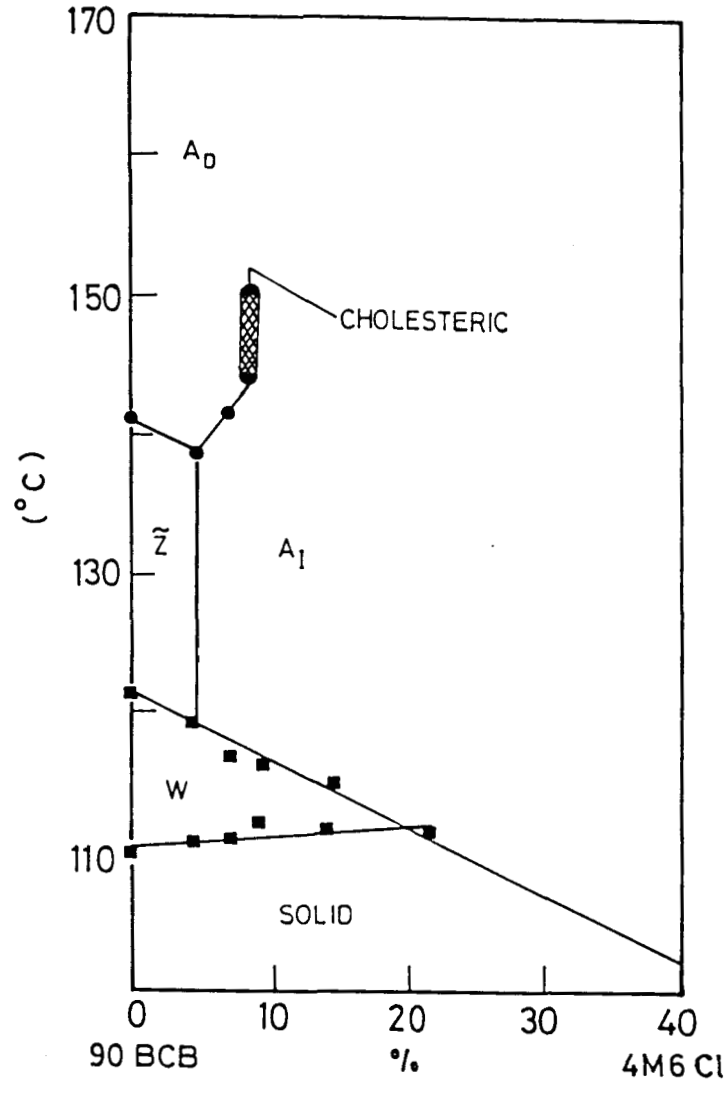

Figure 6.8

Partial phase diagram for mixtures of 90BCB and 4M6Cl showing the cholesteric island which emerges in the vicinity of the smectic A_d - smectic A_1 critical point. The transition from the solid to the liquid-crystal phase called W is the melting transition. $\tilde{Z}$ is a biaxial liquid-crystal phase. The abcissa is weight per cent of 4M6Cl (Ref. 4).

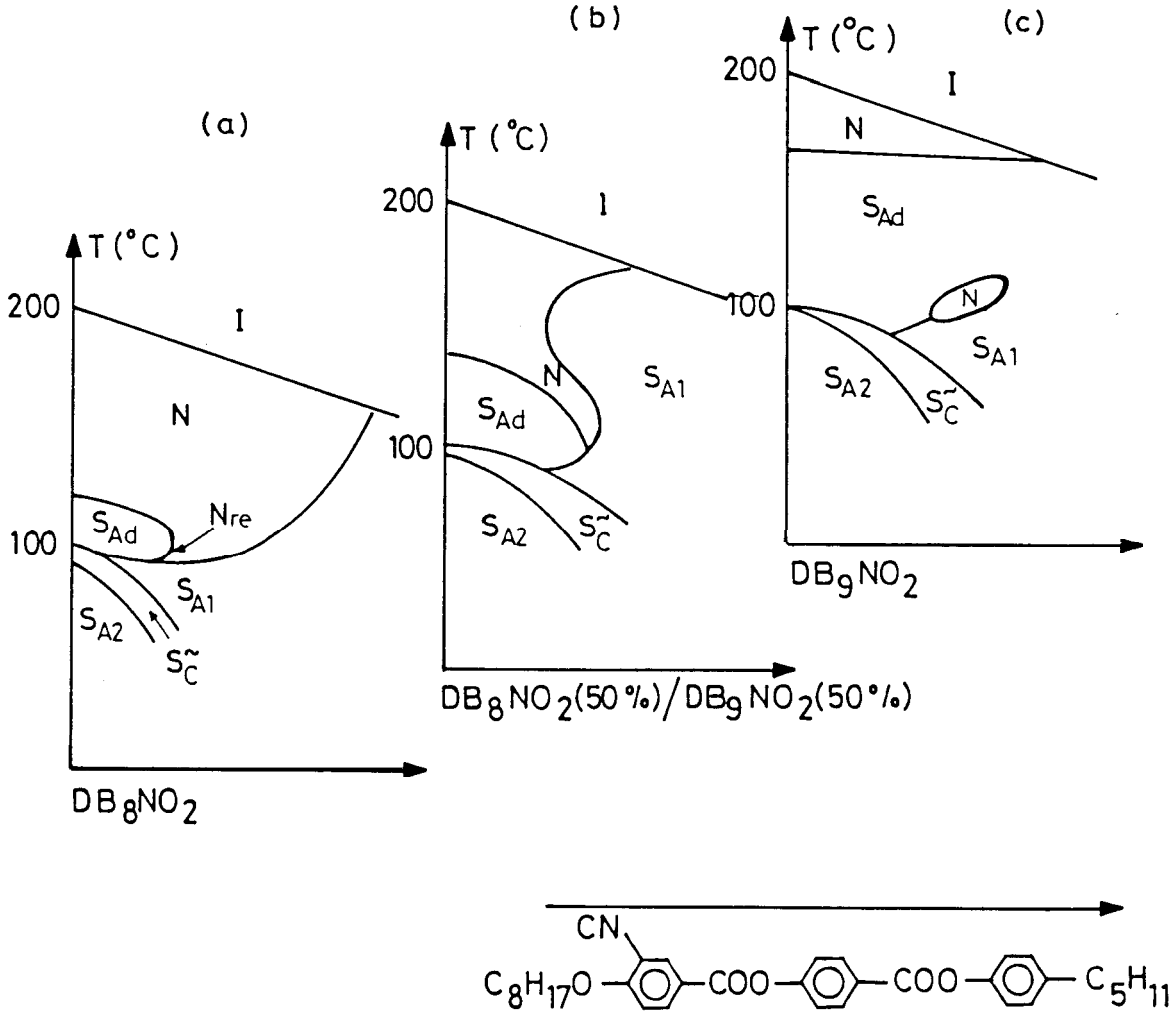

Figure 6.9

Phase diagram of binary systems showing $A_d - N_{re} - A_1$ point and a nematic island as the possible topologies connected with $A_d - A_1$ phase boundary (Ref. 6).

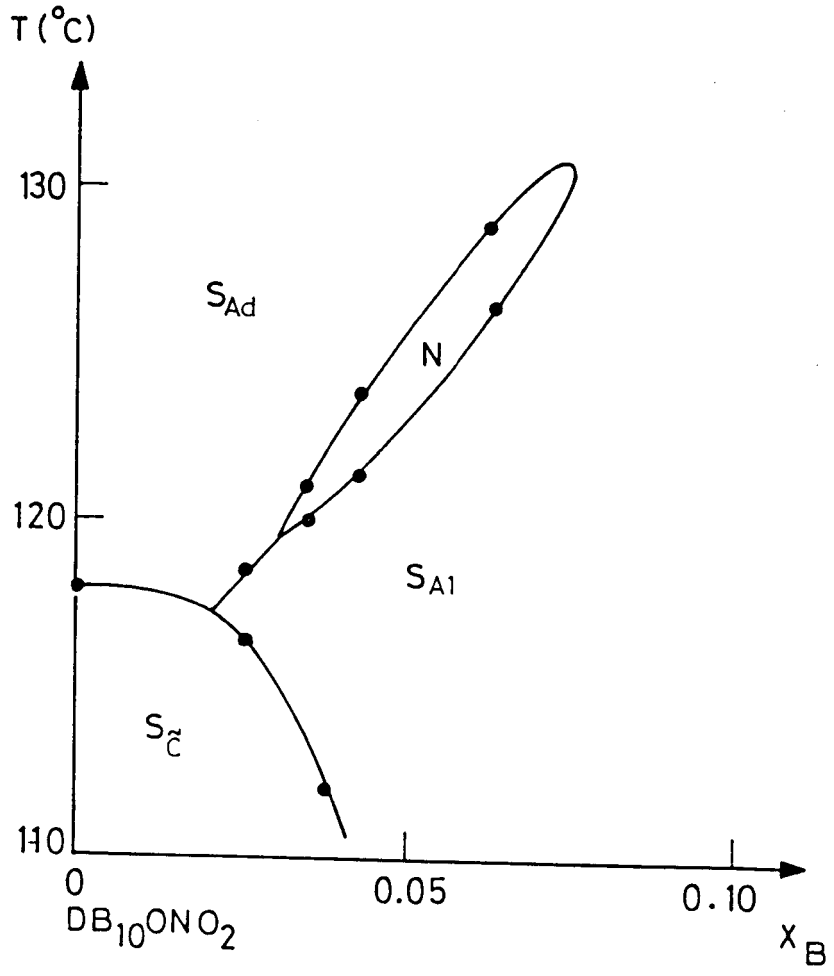

$DB_{10}ONO_2$ (on the left)

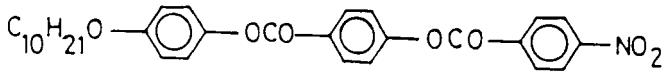

and

"6" (on the right)

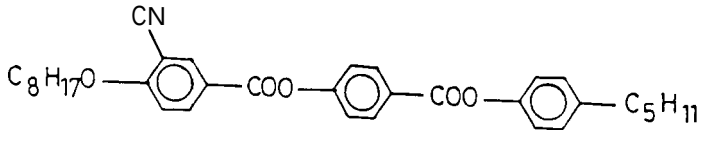

Figure 6.9(d)

Temperature-concentration diagram (at 1 bar) of $DB_{10}ONO_2$ and B exhibiting a nematic island (Ref. 6).

6.4 RESULTS OF STUDIES ON PHASE DIAGRAMS INVOLVING A_d AND A_1 PHASES

In general A_d-A_1 transitions have been seen only when the constituent compounds of a binary system are such that the bridging dipoles in a molecule are opposite to the direction of the strongly polar end group. We undertook study of temperature-concentration diagrams of binary and ternary systems comprising of third and fourth members of the homologous series 4-alkyloxybenzoyloxy-4'-nitroazobenzene (nOBNAB) and 4-nonyloxybenzoyloxy-4'-cyanoazobenzene (9OBCAB), wherein the molecules have bridging dipoles additive with respect to that of the polar end group. The chemical formulae of 3OBNAB, 4OBNAB and 9OBCAB are shown in Fig.6.10 while the transition temperatures of these materials are listed in Table 6.1. The compounds 3OBNAB and 4OBNAB exhibit nematic and smectic A_1 phases, while 9OBCAB exhibits nematic, smectic A_d, reentrant nematic and smectic A_I phases.

The temperature-concentration diagram obtained by mixing 9OBCAB with 4OBNAB is shown in Fig.6.11. As seen from this figure, the A_1 phase of 4OBCAB seems to be miscible with both the A_1 and A_d phases of 9OBNAB. The reentrant nematic phase gets bounded. An important feature of the phase diagram is the steep fall of the N-A_d boundary seen for mixtures close to 9OBCAB. This leads to a broad dip in the concentration range, 70-85%. It

1. 3OBNAB

4 – propyloxybenzoyloxy – 4′ – nitroazobenzene

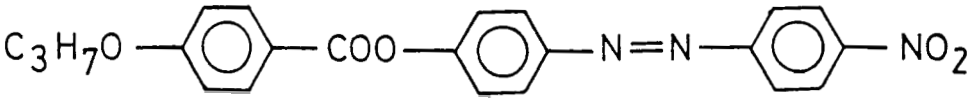

2. 4OBNAB

4 — Butyloxybehzoyloxy – 4′ — nitrozobenzene

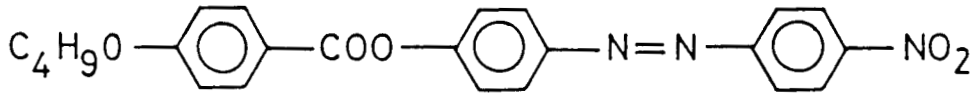

3. 9OBCAB

4 – nonyloxybenzoyloxy – 4′ – cyanoazobenzene

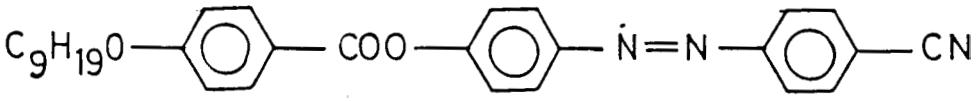

Figure 6.10

Chemical formulae of the materials used.

TABLE 6.1

Transition temperatures (at 1 bar) of 3OBNAB, 4OBNAB and 9OBCAB

Compound	Transition	Temperature (°C)
3OBNAB	Solid - Nematic (K-N)	152.3
	Nematic-Isotropic (N-I)	(124.2)
	Smectic A_1 - Nematic (A_1-N)	291
4OBNAB	Solid-Smectic A_1 (K-A_1)	149
	Smectic A_1 - Nematic (A_1-N)	160.5
	Nematic-Isotropic (N-I)	284
9OBCAB	Solid-Reentrant nematic (K-RN)	91.0
	Reentrant nematic-Smectic A_d (RN-A_d)	116.1
	Smectic A_d - Nematic (A_d-N)	212.4
	Nematic-Isotropic (N-I)	249.5
	Smectic A_1 - Reentrant nematic (A_1 - RN)	(72.4)

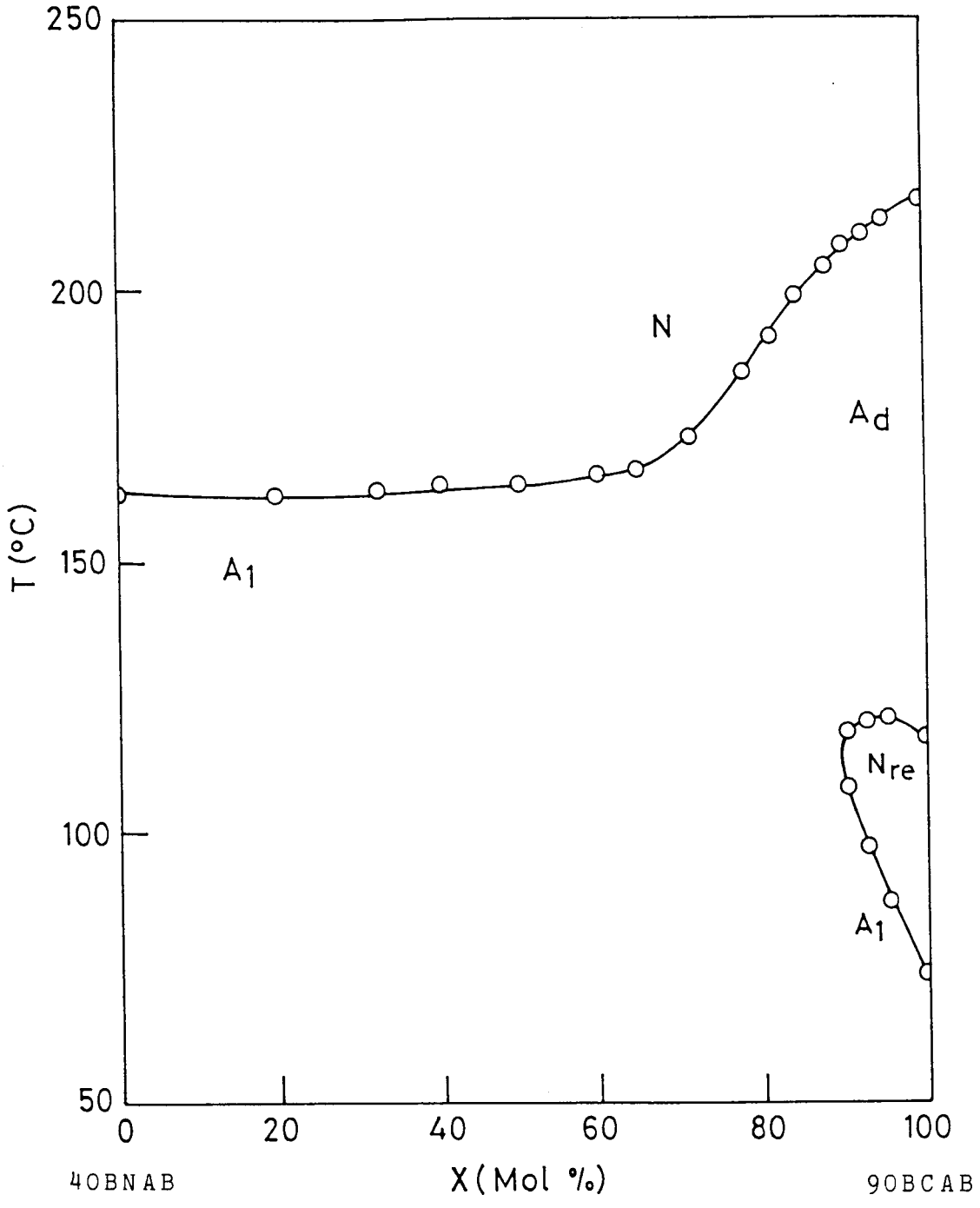

Figure 6.11

T-X diagram of 40BNAB and 90BCAB. X is the mol % of 90BCAB in the mixture.

also appears from the figure that the axis of symmetry of the elliptic (or parabolic) reentrant nematic-smectic A boundary is directed towards this dip on the N-A boundary. These features indicate the possibility of an A_d-A_1 boundary in the smectic region connecting the nematic and reentrant nematic phases. The optical observations on the mixtures in this region (when viewed under a polarising microscope) did not however indicate the existence of an A_d-A_1 transition, possibly because it is sometimes difficult to detect the A-A transitions by observation of textural changes. It may be recalled that Bahr et al.[7] in fact conducted pressure studies on the binary mixture with X = 80% (mole %), the concentration corresponding to the region of broad dip on N-A boundary, with a view to locating A_d-A_1 transition. However, these studies did not yield any positive result but seemed to suggest that A_d phase evolves continuously into A_1 phase. It is more likely that an A_d-A_1 boundary can be induced in the smectic region between the dip on N-A boundary and the tip of the A-RN phase boundary if the dip is made more pronounced and brought closer to the tip of the RN-A boundary on concentration scale. In order to achieve this we studied three T-X diagrams with HK_9 as one component (B) and binary mixtures of 3OBNAB and 4OBNAB as another component (A). The concentrations of 3OBNAB/4OBNAB system used as a constituent in making the different ternary systems along with the transition temperatures are listed in Table 6.2. Figures 6.12 - 6.14 represent the three ternary phase diagrams

TABLE *6.2*

Concentrations and transition temperatures (in °C) of the 3OBNAB/4OBNAB binary systems used as one of the constituents in the ternary systems. The other constituent is 9OBCAB in every case (see text).

System	Transition temperatures	
	A - N	N - I
(i) 79% 3OBNAB/21% 4OBNAB	135.7	290
(ii) 85% 3OBNAB/15% 4OBNAB	130.9	290.4
(iii) 95% 3OBNAB/5% 4OBNAB	127.3	290.8

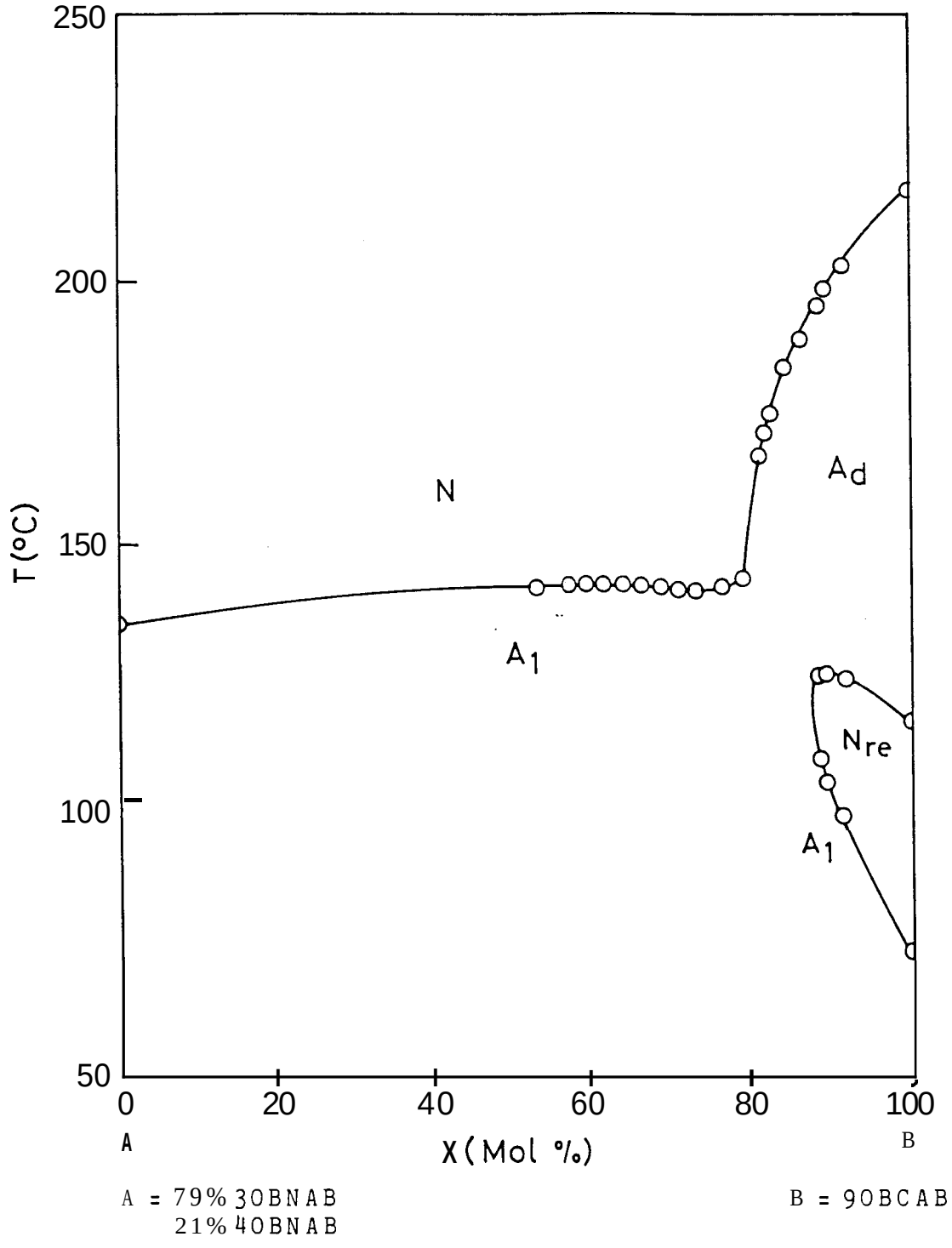

Figure 6.12

Temperature-concentration diagram of A and B. X is the mol % of B in the mixture.

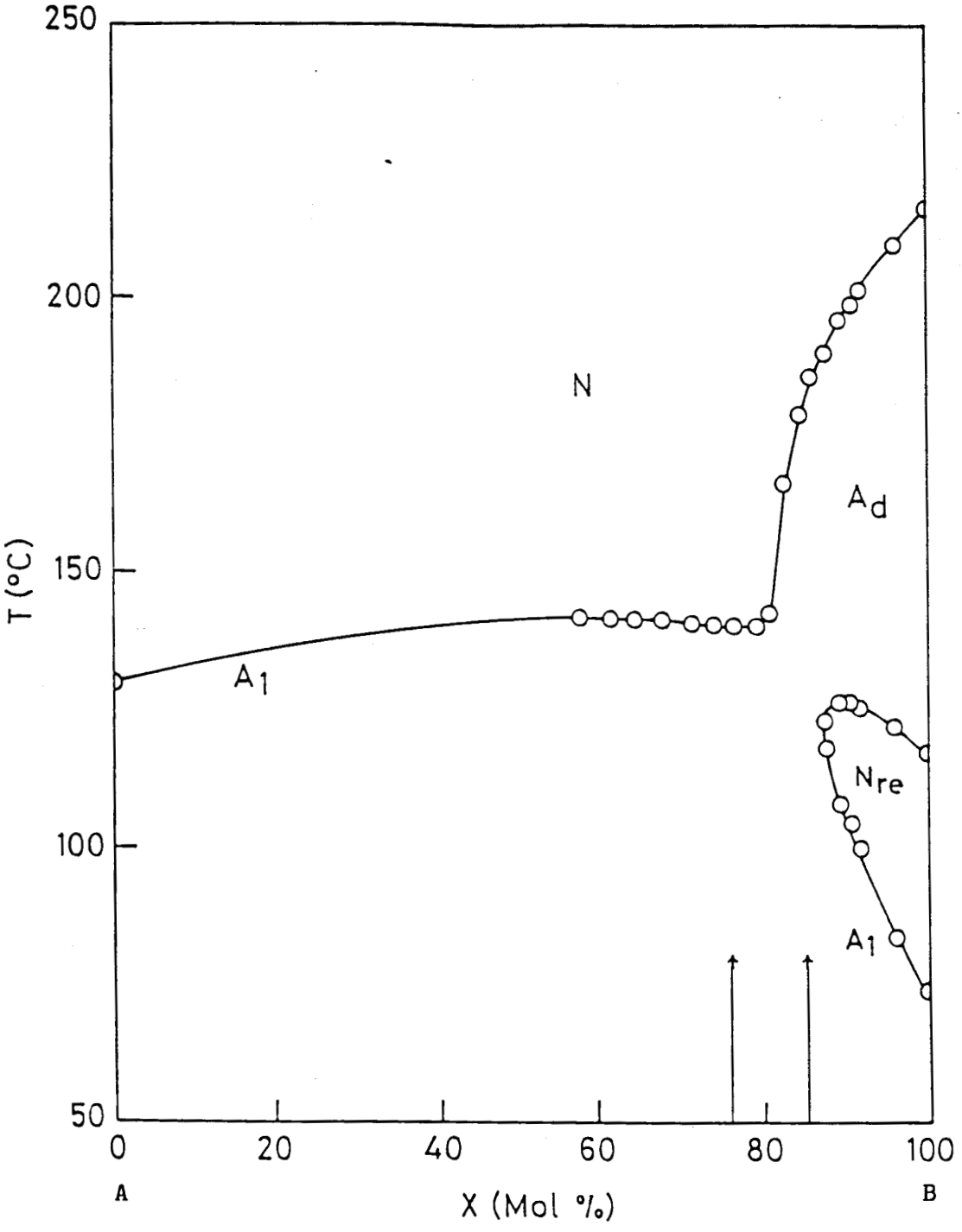

A = 85% 30BNAB
15% 40BNAB

B = 90BCAB

Figure 6.13

Temperature-concentration diagram of A and B. X is the mol % of B in the mixture. The vertical lines indicate the two ternary mixtures, X = 75.8% and 85% of B, for which high resolution Xray diffraction studies are conducted.

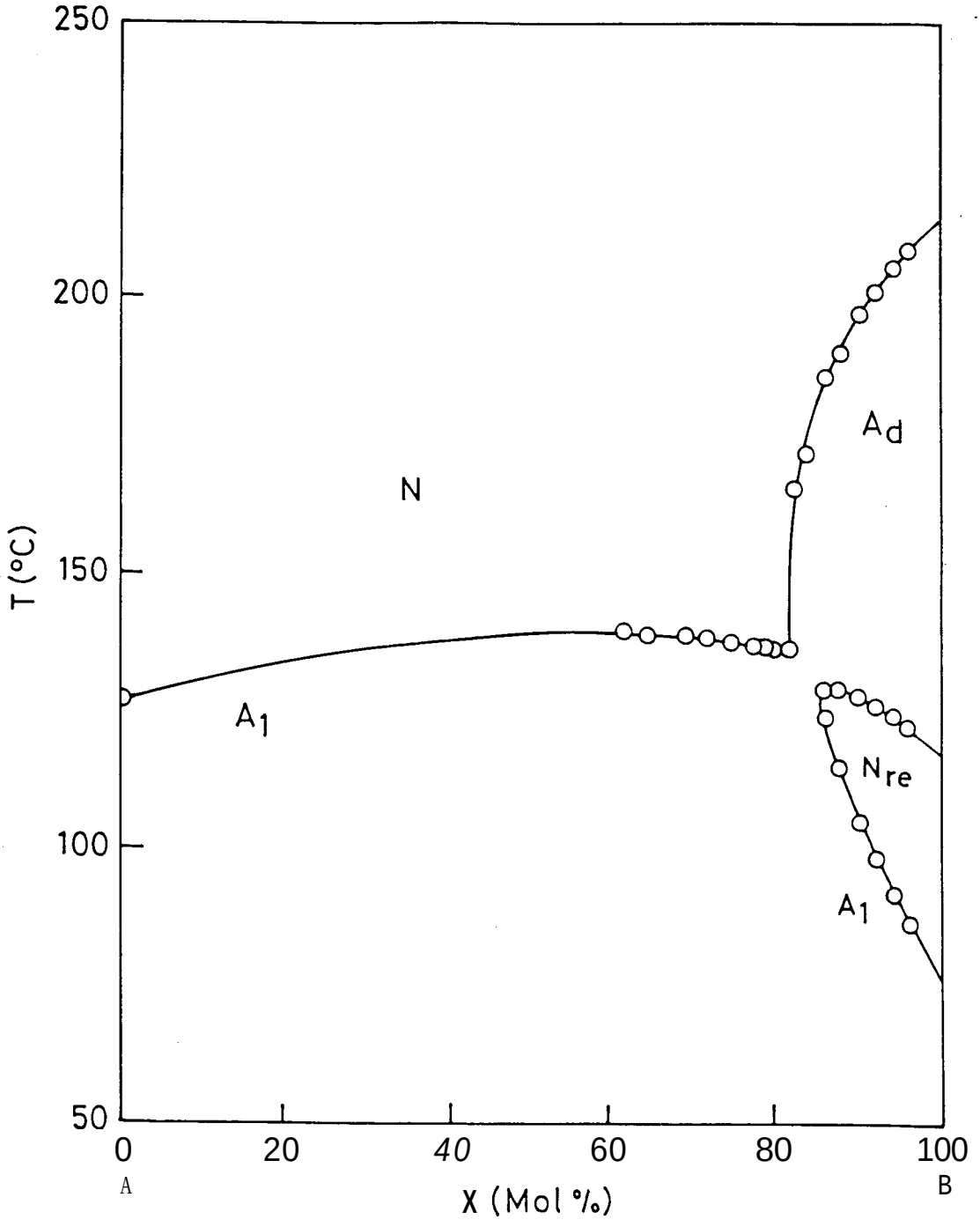

A = 95% 3OBNAB
5% 4OBNAB

B = 9OBCAB

Figure 6.14

Temperature-concentration diagram of A and B. X is the mol % of B in the mixture.

obtained in this manner. As expected, increasing 3OBNAB component in A makes the N-A boundary much steeper which makes the dip or cusp on the N-A boundary more pronounced, when compared to the features in the binary T-X diagram of 4OBNAB and 9OBCAB. Also, with the increasing 3OBNAB concentration the tip of the "bubble-like" reentrant nematic region is pulled towards the cusp of the N-A boundary and we see a "constricted smectic region" separating the nematic and reentrant regions. Finally, when 9OBCAB is mixed with 3OBNAB, the T-X diagram obtained (Fig.6.15) is dramatically different from the ones discussed so far. The A_d phase of 9OBCAB is now completely separated from the A_1 phase of 3OBNAB with a small channel of nematic phase connecting the nematic and reentrant nematic phases. The A_1 phases of 3OBNAB and 9OBCAB are however still miscible.

As pointed already, the steep curvature of the N-A boundary with a pronounced cusp, and the close proximity of the cusp with the tip of the reentrant nematic-smectic A boundary (seen in Fig. 6.14) do strongly suggest the existence of a A_d-A_1 phase boundary in the narrow smectic region between nematic and reentrant nematic phases. This A_d-A_1 boundary may either connect the nematic and reentrant nematic boundaries or may, by connecting either of them, terminate as a critical point at the other end. To locate the A_d-A_1 boundary and also a possible critical point terminating it, we conduc-

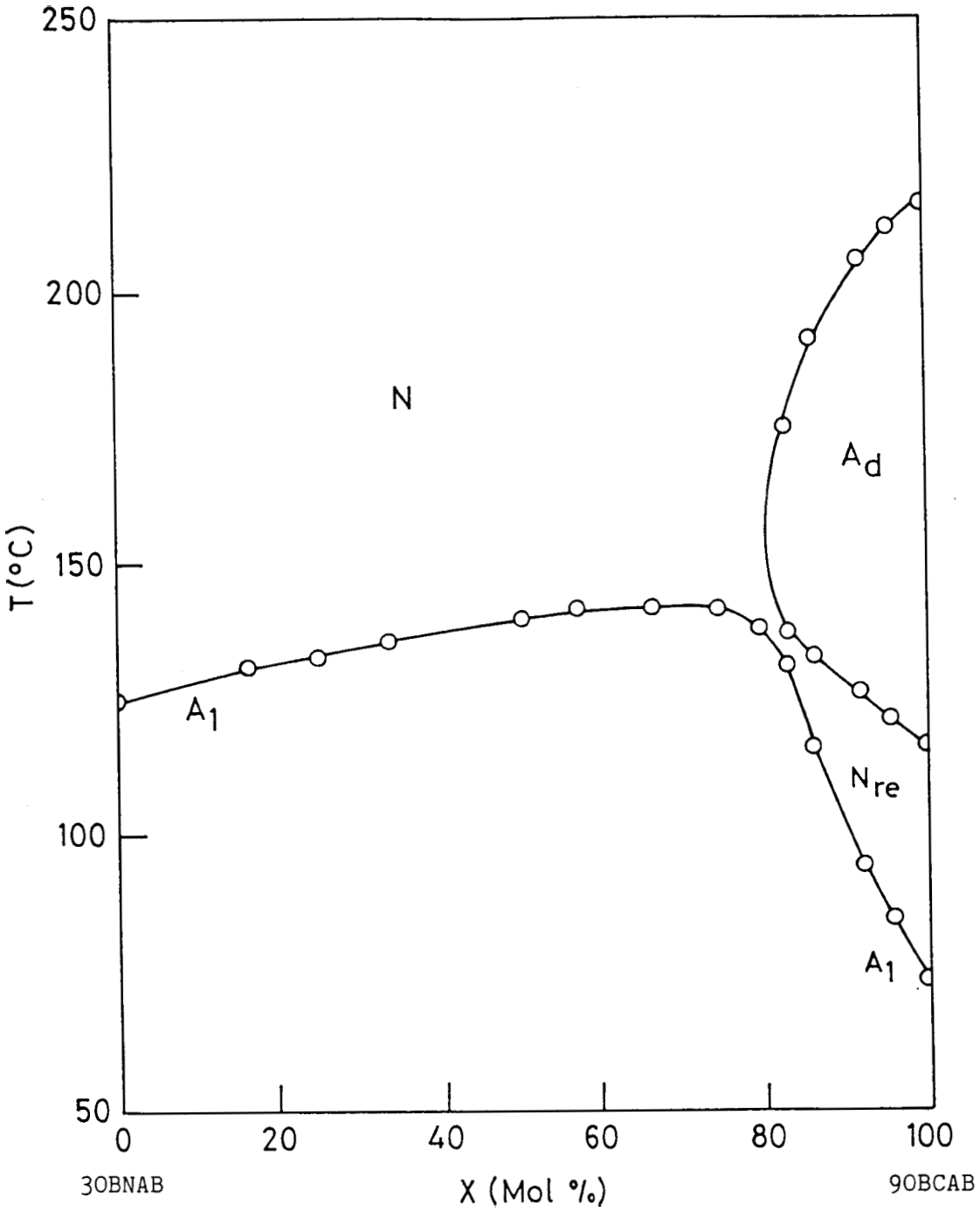

Figure 6.15

Binary T–X diagram of 30BNAB and 90BCAB. X is the mol % of 90BCAB in the mixture

ted high resolution Xray diffraction experiments on two ternary systems marked in Fig.6.13: (i) X = 75.8% and (ii) X = 85% of B in the system (where A = 85% 3OBNAB - 15% 4OBNAB binary system and B is 9OBCAB). The 85% ternary mixture shows nematic and smectic phases on cooling from the isotropic phase when viewed under polarising microscope. We could not detect any A_d-A_1 transition. The sample was sealed in a Lindemann capillary of 0.5 mm diameter and 17-18 mm in length. The sample alignment and data collection using a computer controlled Xray diffractometer was done as explained in detail in chapter II. These data are represented by Fig.6.16a. As is observed from this figure, the layer spacing of the A_d phase at 145°C is 34.75 Å and on decreasing the temperature, the layer spacing is found to decrease gradually right up to 115°C which is well within the low temperature smectic A_1 phase. The d/ℓ ratio which is 1.044 at 145° decreases to 1.014 at 115°C. The absence of a discontinuity in layer spacing variation shows that the expected A_d-A_I transition does not exist and suggests on the other hand a continuous evolution of A_d phase into the A_I phase. The Xray diffraction data on the mixture of concentration X=75.8%, which exhibits only nematic and smectic A_I phases are represented in the Fig.6.16b. The layer spacing of the monolayer smectic A (A_I) phase which is about 31.25 Å at t=138°C decreases gradually on decreasing the temperature, the d/ℓ ratio which is

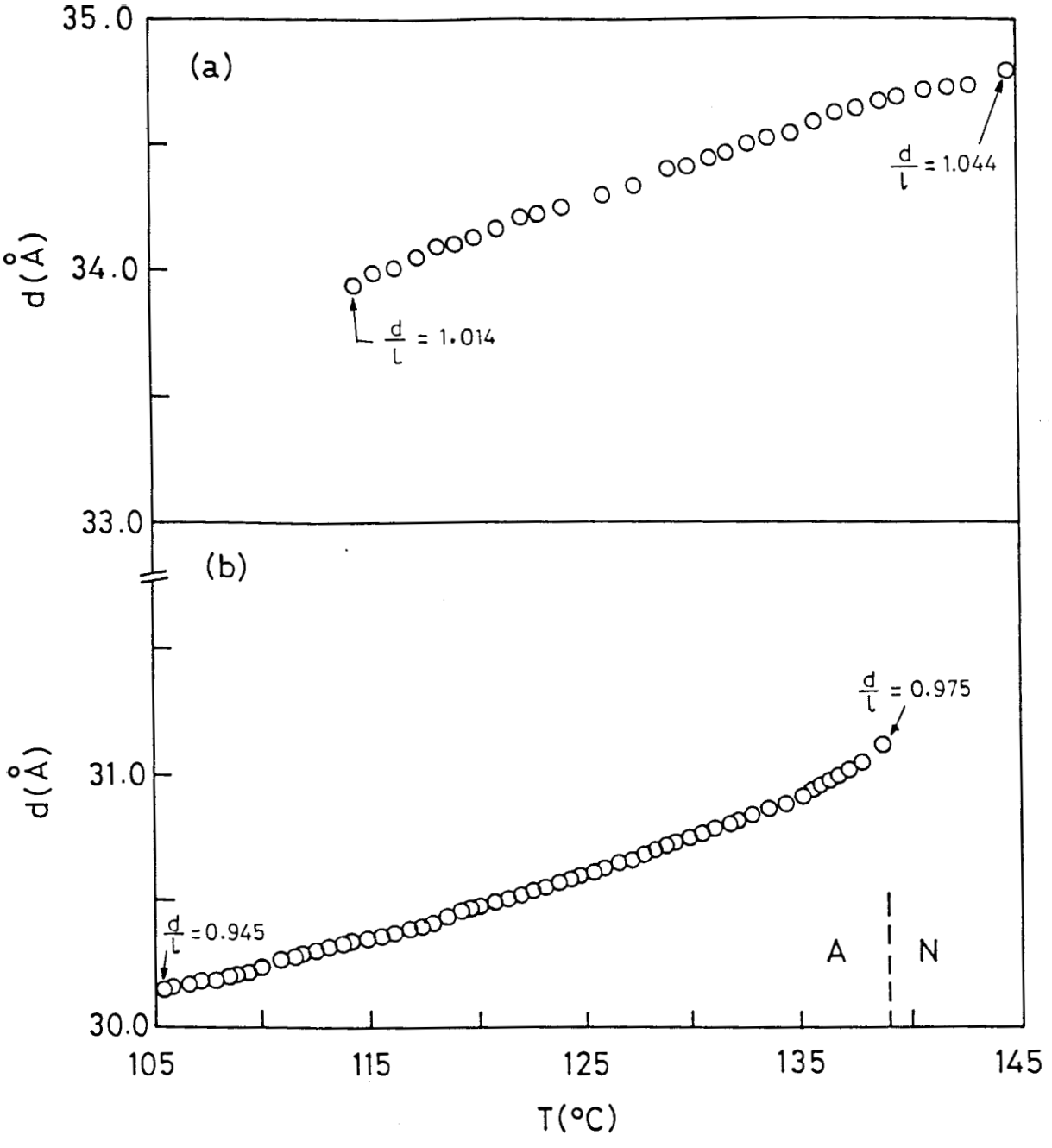

Figure 6.16

Variation of layer spacing with temperature for (a) 85% and (b) 75.8 % of 9OBCAB in the ternary mixtures.

0.975 at 138°C decreasing to 0.945 at 105°C.

The non-observation of A_d-A_1 boundary and hence a critical point terminating it in the temperature-concentration plane of ternary systems described above may suggest that the smetic region in the vicinity of the tip of the RN-A phase boundary (Fig.6.12) may correspond to the critical region around the nematic island shown in the theoreticaly predicted phase diagram (Fig.6.1). The "main domain" nematic region seen in the experimental phase diagram (Fig.6.11) is expected to be far away from the nematic island and hence is not seen in the theroetical diagram (Fig.6.1). The variation of the concentration of 3OBNAB in the component A has resulted only in bringing the 'main nematic domain' closer to the 'nematic island' with the intervening smectic region being the critical region (where the A_d phase evolves continuously into A_1 phase) (Fig.6.12-6.14), a situation that still fits the theoretical prediction. The T-X diagram (Fig.6.15) for the binary system 3OBNAB/9OBCAB with the two smectic regions (A_d region and A_1 region) separated by a constricted nematic gap connecting the nematic phase and the reentrant nematic phase, bears resemblance in part to the theoretical phase diagram (Fig. 6.7) wherein the nematic island merges with the main domain (nematic regions) separating the two smectic phases. The topological features of A_d- RN and RN-A_1 boundaries beyond 9OBCAB being inaccessible, we are unable to reproduce

that part of the phase diagram (Fig.6.7) which shows the A_d-A_l boundary connected to nematic island with two nematic phases, N_d and N_l, leading to two critical end points (A,B) and a critical point (C) for N_d-N_l boundary.

Thus, from our experimental results on ternary and binary systems involving 3OBNAB, 4OBNAB and 9OBCAB, we have been successful in reproducing, although qualitatively, some of the theoretical phase diagrams predicted theoretically by Prost and Toner. The A_d-A_l boundary and the critical point terminating it have been inaccessible in our systems. Clearly, a careful study of a variety of phase diagrams comprising of components exhibiting A_d-A_1 boundary and also the continuous evolution of A_d to A_l (critical region) phases, supported by very high resolution Xray and calorimetric data, is required to establish experimentally the theoretical predictions concerning the existence of an A_d-A_1 or nematic-nematic critical point.

REFERENCES

I B.R.Ratna, R. Shashidhar and V.N.Raja, Phys. Rev. Lett., 55, 1476 (1985)

2 J. Prost and J. Toner, Phys. Rev. A (in press)

3 P.Barois, J. Prost and T.C.Lubensky, J. de Phys., 46, 391 (1985)

4 W. Helfrich, J. de Phys., 39, 1199 (1978)

5 P.E.Cladis and H.R.Brand, Phys. Rev. Lett., 52, 2210 (1984)

6 F.Hardouin, M.F.Achard, Nguyen Huu Tinh and G.Sigaud, Mol. Cryst. Liq. Cryst. Lett., 3, 7 (1986)

7 C. Bahr, G. Heppke and R.Shashidhar, Z. Naturforsch., 40a, 1311 (1985)